Generalized hydrodynamics, quasiparticle diffusion, and anomalous local relaxation in random integrable spin chains

Utkarsh Agrawal,[1] Sarang Gopalakrishnan,[2,3] and Romain Vasseur[1]

[1]*Department of Physics, University of Massachusetts, Amherst, Massachusetts 01003, USA*

[2]*Department of Physics and Astronomy, CUNY College of Staten Island, Staten Island, New York 10314, USA*

[3]*Physics Program and Initiative for the Theoretical Sciences, The Graduate Center, CUNY, New York, New York 10016, USA*

(Received 21 March 2019; revised manuscript received 29 April 2019; published 15 May 2019)

We study the nonequilibrium dynamics of random spin chains that remain integrable (i.e., solvable via Bethe ansatz): because of correlations in the disorder, these systems escape localization and feature ballistically spreading quasiparticles. We derive a generalized hydrodynamic theory for dynamics in such random integrable systems, including diffusive corrections due to disorder, and use it to study nonequilibrium energy and spin transport. We show that diffusive corrections to the ballistic propagation of quasiparticles can arise even in noninteracting settings, in sharp contrast to clean integrable systems. This implies that operator fronts broaden diffusively in random integrable systems. By tuning parameters in the disorder distribution, one can drive this model through an unusual phase transition, between a phase where all wave functions are delocalized and a phase in which low-energy wave functions are quasilocalized (in a sense we specify). Both phases have ballistic transport; however, in the quasilocalized phase, local autocorrelation functions decay with an anomalous power law, and the density of states diverges at low energy.

DOI: 10.1103/PhysRevB.99.174203

I. INTRODUCTION

The study of the dynamics of isolated, many-body quantum systems far from thermal equilibrium has attracted a lot of attention recently, fueled by recent experimental developments on ultracold atoms [1–3], trapped ions [4–6], nitrogen-vacancy centers [7,8], and superconducting qubits [9] platforms. Addressing questions about nonequilibrium transport, thermalization, and far-from-equilibrium dynamics poses notable challenges for theory as they are not susceptible to the general principles and methods that govern the physics of low-energy, equilibrium systems.

With the notable exception of many-body localized systems [10–12], generic many-body systems are expected to be "chaotic" and to thermalize under their own dynamics [13]. This process can be understood as the scrambling of quantum information as it becomes nonlocal and inaccessible to physical, local measurements. After a local equilibration regime, thermalizing systems can be well described by classical hydrodynamic equations associated with conserved quantities—typically, energy, particle number, and momentum. These hydrodynamic equations describe the evolution of the system from local to global equilibrium. Another class of systems that escapes thermalization in the traditional sense is quantum integrable systems, including experimentally relevant examples such as the Heisenberg antiferromagnet and the Lieb-Liniger Bose gas in one dimension [2,3,14]. Such systems have stable quasiparticle excitations even at high temperature and they possess an extensive number of conserved quantities which strongly constrain their dynamics and prevent them from thermalizing like generic chaotic systems [15–25]. However, contrary to many-body localized systems, integrable systems do thermalize in a generalized sense, as they eventually reach a maximum entropy steady state described by a generalized Gibbs ensemble (GGE) [3,26–28]. Such steady states can exhibit nonzero currents and are commonly referred to as nonequilibrium steady states (NESS) in the literature [11,29], even though they are natural equilibrium states for integrable systems.

A major step in understanding the nonequilibrium dynamics of quantum integrable systems was the formulation of what is now known as "generalized hydrodynamics" (GHD) [30,31], which are Euler hydrodynamics equations (zeroth-order hydrodynamics) obtained in the large space-time limit where the system is locally in equilibrium. While the prospect of solving infinitely many hydrodynamic equations (one for each conserved quantity in the system) originally appeared daunting, GHD can be conveniently formulated in the basis of quasiparticle excitations: in that language, they can be naturally interpreted as describing a semiclassical gas of solitons (quasiparticles) [32–35]. The key ingredient of GHD is the effective group velocity v^{eff} of the quasiparticles [30,31,36], which depends on the density of all the other quasiparticles in the presence of interactions: at the semiclassical level, quasiparticle wave packets pick up a phase shift when they collide, leading to a Wigner time delay. This approach was successfully applied to two-reservoir setups [30,31] and, more generally, to locally equilibrated inhomogeneous initial states [37–39], and has helped addressing a number of key questions in the field concerning Drude weights [34,40–43], external potentials and traps [44–46], correlation functions [47], entanglement dynamics [48], or even large-deviation functions [49].

The GHD framework was recently generalized to include diffusive effects in interacting integrable models

[50–53]—corresponding to "first-order" or Navier-Stokes hydrodynamics, with important consequences for the nature of spin transport in XXZ spin chains [52,53]. In particular, Ref. [50] provided a general exact expression of the "diffusion matrix" of the quasiparticles using a form factor expansion of the Kubo formula. Intuitively, diffusive corrections can be seen to arise as follows [51]: the effective velocity of a given quasiparticle depends on the density of quasiparticles in a mean-field fashion that ignores fluctuations; reintroducing thermal fluctuations naturally leads to a diffusive broadening of quasiparticle trajectories in a generic GGE state. Two key ingredients are needed for such diffusive corrections to be present: density-dependent velocities and thermal fluctuations (nonzero entropy states). This immediately implies that in noninteracting integrable models where the group velocity is obtained from band theory and is independent of density, there should be no diffusion [54]. For noninteracting systems, it is thus natural to expect that the lowest-order correction to ballistic GHD comes from higher-order derivative terms, which lead to $t^{1/3}$ spreading governed by the Airy kernel (see Ref. [55] and references therein). Clearly, such higher-order corrections are subleading in the presence of diffusive $t^{1/2}$ spreading.

In this paper, we study a class of integrable random spin chains which support diffusive corrections even in the absence of interactions. These spin chains are a special limit of a more general class of random interacting spin chains that remain integrable. In one-dimensional free-particle problems, disorder generically leads to Anderson localization. Though Anderson localized systems are "integrable" in a sense, here we will use the term "integrability" exclusively to refer to Bethe-ansatz solvable systems with stable ballistically propagating quasiparticles. There are examples of integrable models with impurities [56–58] where disorder is correlated in such a way that integrability in this sense is preserved. Such systems were recently shown to exhibit ballistic transport even at strong disorder in Ref. [58]. It is natural to expect such random systems to exhibit diffusive corrections to ballistic transport even without interactions, as quasiparticles scatter off random static impurities and thus undergo biased random walks. These models illustrate that whereas noninteracting systems are often said to be always integrable, integrability for a random system leads to correlated disorder that can allow one-dimensional random systems to escape Anderson localization. Correlated disorder can then lead to ballistic transport and diffusive corrections, even in the absence of interactions. Although most states in these models are only weakly affected by the disorder, quasiparticle states near energy $|E| = 0$ have properties that are sensitive to the tails of the disorder distribution. We find disorder distributions for which these quasiparticles have vanishing velocities, so that the behavior of local autocorrelation functions is anomalous—neither ballistic nor diffusive. We find that the onset of anomalous behavior in the disorder-averaged autocorrelation functions is associated with the onset of a divergence in the density of states at zero energy, as well as a form of quasilocalization of the low-energy wave functions that we discuss below. We compute this anomalous relaxation exponent using GHD. There are strong local correlations between the density of states and the quasiparticle velocity, as both are dominated by rare regions; our work shows how GHD can be adapted to incorporate these rare region effects.

In this work, we propose a hydrodynamic theory to describe such random integrable spin chains, including diffusive corrections due to disorder. The plan of this paper is as follows: in Sec. II, we recall the definition of a family of random integrable spin chains recently studied in Ref. [58] and we briefly review their thermodynamics. We then formulate a coarse-grained GHD theory for the dynamics of such systems in Sec. III, with an emphasis on diffusive corrections due to disorder in noninteracting settings (for which disorder is the only possible source of diffusive corrections). This framework is applied to study nonequilibrium spin and energy transport, and the predictions are compared to numerical results in Sec. IV. Transport is dominated by fast quasiparticles with energies well away from $|E| = 0$. We turn, in Sec. V, to a more careful discussion of states near $|E| = 0$. For these states, we find a quasilocalization transition; in the quasilocalized regime, low-energy wave functions consist of a few local peaks, quasiparticle velocities vanish, and the density of states diverges in the $|E| \to 0$ limit. Consequences for operator spreading and scrambling are briefly discussed in Sec. VI, and a discussion and outlooks for future works are gathered in Sec. VII.

II. RANDOM INTEGRABLE SPIN CHAINS

In this section, we introduce a family of random integrable spin chains, closely following Ref. [58], and we briefly review their thermodynamic Bethe-ansatz solution.

A. Hamiltonian

Let us consider a random XXZ spin-$\frac{1}{2}$ chain $H = \sum_i J_i[\vec{\sigma}_i.\vec{\sigma}_{i+1}]_{\Delta_i}$, where $[\vec{\sigma}_j.\vec{\sigma}_k]_{\Delta_i}$ is a shorthand notation for $\sigma_j^x\sigma_k^x + \sigma_j^y\sigma_k^y + \Delta_i(\sigma_j^z\sigma_k^z - 1)$. In the clean (homogeneous) case, this model is integrable, but the introduction of disorder immediately breaks integrability and leads to a model that is either chaotic or many-body localized [59,60]. However, it is possible to preserve integrability [56–58] by introducing next-to-nearest-neighbor interactions and by carefully choosing the inhomogeneous couplings,

$$\begin{aligned} H = \sum_{j=1}^{L/2} & J_{2j}^{(1)}\left([\vec{\sigma}_{2j-1}.\vec{\sigma}_{2j}]_{\Delta_{2j}} + [\vec{\sigma}_{2j}.\vec{\sigma}_{2j+1}]_{\Delta_{2j}}\right) \\ & + K_{2j}\left\{[\vec{\sigma}_{2j}.(\vec{\sigma}_{2j-1}\times\vec{\sigma}_{2j+1})]_{\Delta_{2j}^{-1}} + \Delta_{2j}^{-1}\right\} \\ & + J_{2j}^{(2)}(\vec{\sigma}_{2j-1}.\vec{\sigma}_{2j+1} - 1). \end{aligned} \tag{1}$$

The first line of the Hamiltonian corresponds to an XXZ interaction, while the last line is an isotropic Heisenberg interaction. The middle line is more unusual, as it involves three spins. The parameters in the Hamiltonian are given by

$$\begin{aligned} J_{2j}^{(1)} &= \frac{\sin^2\eta\,\cosh\xi_{2j}}{\sin^2\eta + \sinh^2\xi_{2j}}, \quad J_{2j}^{(2)} = \frac{\cos\eta\,\sinh^2\xi_{2j}}{\sin^2\eta + \sinh^2\xi_{2j}}, \\ K_{2j} &= \frac{\sin\eta\cos\eta\,\sinh\xi_{2j}}{\sin^2\eta + \sinh^2\xi_{2j}}, \quad \Delta_{2j} = \frac{\cos\eta}{\cosh\xi_{2j}}, \end{aligned} \tag{2}$$

with ξ_{2j} a random coupling, while η is an overall global parameter that parametrizes the interaction strength. For $\xi_{2j} = 0$, one recovers the usual XXZ spin chain. A remarkable feature of this model is that it remains integrable for any choice of the inhomogeneous couplings ξ_{2j}. Away from the zero-energy limit, the properties of this model are insensitive to details of the disorder distribution. Therefore, except as specified below (i.e., in Sec. V and subsequently), we will take the ξ_{2j} couplings to be random variables drawn from the Gaussian distribution,

$$P(\xi) = \frac{1}{\sqrt{2\pi W^2}} e^{-\xi^2/2W^2}. \tag{3}$$

Later, we will also consider the exponential distribution,

$$P(\xi) = \frac{\phi}{2} e^{-\phi|\xi|}, \tag{4}$$

for which a sharp quasilocalization transition exists.

We will be especially interested in the special point $\eta = \pi/2$. For this value of η, the XXX part of the Hamiltonian is set to zero, leaving behind a random XX model with three spin interactions,

$$H = \sum_{j=1}^{L/2} \left\{ \frac{1}{\cosh \xi_{2j}} \sum_{\alpha=x,y} \left[\sigma^\alpha_{2j-1}\sigma^\alpha_{2j} + \sigma^\alpha_{2j}\sigma^\alpha_{2j+1}\right] + \tanh(\xi_{2j})\left[\sigma^y_{2j-1}\sigma^z_{2j}\sigma^x_{2j+1} - \sigma^x_{2j-1}\sigma^z_{2j}\sigma^y_{2j+1}\right] \right\}. \tag{5}$$

The above Hamiltonian can be diagonalized via Jordan-Wigner transformation, reducing it to a free-fermion model:

$$H = -\sum_{j=1}^{L} \frac{2}{\cosh(\xi_j)} (c^\dagger_j c_{j+1} + \text{H.c.}) + \sum_{j=1}^{L/2} 2i\tanh(\xi_{2j})(c^\dagger_{2j-1}c_{2j+1} - \text{H.c.}), \tag{6}$$

where the ξ_j's are random parameters used in Eq. (1), extended to odd sites via relation $\xi_{2j-1} = \xi_{2j}$. We use periodic boundary conditions for the fermions for an even number of sites. While noninteracting and disordered, this model was shown to escape Anderson localization, in Ref. [58], and to exhibit ballistic transport of conserved quantities. It is then natural to ask if transport properties of this model can be captured using generalized hydrodynamic equations, properly adapted to deal with the quenched disorder. If so, it is natural to expect disorder to lead to new hydrodynamic effects, such as diffusion. In the following, we will mostly focus on the special point $\eta = \pi/2$ [Eqs. (6) and (5)], though we expect our approach to generalize to any value of η. This will be convenient as the free-fermion representation of this model allows one to easily simulate numerically the nonequilibrium dynamics of this system and, more importantly, the absence of interactions will allow us to isolate the effect of disorder on diffusion.

B. Thermodynamics

The model introduced above admits an exact solution by Bethe ansatz. In the following, we very briefly review the thermodynamic Bethe-ansatz (TBA) approach to integrable systems, with the main goal of introducing some notation and language that will be used in the remainder of this paper [61].

The solutions of the Bethe equations are expressed in terms of quasimomenta or rapidities, and as one takes the thermodynamic limit, one introduces a density of allowed quasimomenta $\rho^T(\lambda)$, corresponding to a total density of states. In general, we will also introduce an additional discrete quasiparticle label j; for XXZ-like spin chains, j is known as the string index. Each allowed quasimomentum state can be occupied or not in a given macrostate, so one defines the hole density ρ^h_j and the density of occupied states (quasiparticle density) ρ_j, and we have $\rho^T(\lambda) = \rho_j(\lambda) + \rho^h_j(\lambda)$ by definition. The particle density together with hole density fully characterize the state of the system. The expectation value of a conserved quantity in such a state can be written as $Q = \int \rho_j(\lambda) q_j(\lambda) d\lambda$, where $q(\lambda)$ is the single-particle charge eigenvalue of the string of type j with quasimomentum λ.

Thermodynamic equilibrium properties can be computed by writing the entropy and energy in terms of ρ and ρ^h, and then maximizing the free energy as usual for a given set of Lagrange multipliers corresponding to a GGE. This leads to the so-called Yang-Yang equation [62]. The Yang-Yang equation together with the Bethe equation are enough to fully determine the quasiparticle densities ρ_j and ρ^h_j, corresponding to a given GGE state. In the following, we will promote these variables locally by assuming local (generalized) equilibrium.

III. GENERALIZED HYDRODYNAMICS APPROACH

We now formulate a hydrodynamic description of such random integrable systems. The evolution of chaotic quantum systems from local to global equilibrium is described by the framework of hydrodynamics. In that regime, one imagines chopping off the system into hydrodynamic cells that are big enough to assume equilibrium within each cell, but very small compared to the total system size. This separation of scales allows one to assume local equilibrium, where Lagrange multipliers such as temperature or chemical potential are allowed to depend on position and time.

There is one hydrodynamic equation per conserved quantity in the system—any other information about the system is "scrambled" by the quantum dynamics into nonlocal entanglement that is not measurable by local observables. For each conserved quantity $Q_n = \sum_x q_n(x)$, we can write a continuity equation,

$$\partial_t q_n(x,t) + \partial_x j_n(x,t) = 0, \tag{7}$$

where we restricted ourselves to one spatial dimension. Assuming local equilibrium then leads to a relation $j_n = F_n[\{q_m\}]$ between the currents j_n and the conserved charges q_m at a given position x: this relation is an equilibrium property and gives rise to *Euler* hydrodynamic equations that govern ballistic transport properties. More generally, one can perform a gradient expansion of the (expectation value of the) currents in terms of the charges, where contributions to the currents coming from gradient terms $D_{nm}\partial_x q_m$ correspond to diffusive contributions to hydrodynamics (see, e.g., [63]). The diffusion constants D_{nm} are not entirely given by equilibrium properties and have to be determined by other means such as the

Kubo formula or by using kinetic theory calculations. Once the transport coefficients characterizing the relation between currents and charges are known, hydrodynamics provides a simple set of classical, partial-differential equations that govern the nonequilibrium dynamics of the system.

A. Generalized hydrodynamics

The hydrodynamic framework summarized above is completely general and it was successfully applied to integrable systems [30,31]: the resulting framework is now known as *generalized hydrodynamics* (GHD), as it describes systems in local GGE equilibrium. There, local equilibrium is characterized by the densities $\rho_{j,\lambda}(x,t)$, $\rho^h_{j,\lambda}(x,t)$, with the charges $q_n(x) = \sum_j \int q_{n,j,\lambda}\rho_{j,\lambda}(x)d\lambda$ and currents $j_n(x) = \sum_j \int v^{\rm eff}_{j,\lambda}(x) q_{n,j,\lambda}\rho_{j,\lambda}(x)d\lambda$ [ignoring gradient (diffusive) corrections]. $v^{\rm eff}_j$ is interpreted as a group velocity which is a functional of the quasiparticle density in general. The continuity equations for the conserved charges then imply a continuity equation for the quasiparticle density [30,31],

$$\partial_t \rho_{j,\lambda} + \partial_x\left(v^{\rm eff}_{j,\lambda}\rho_{j,\lambda}\right) = 0. \tag{8}$$

For a noninteracting system, $v^{\rm eff}_j$ is independent of ρ_j. In that case, in clean systems, diffusive corrections to (8) are believed to be absent.

We now turn to our specific example (5), which is noninteracting in the fermionic language. Recall that in the noninteracting limit, $\eta = \pi/2$ in Eq. (2). In this limit, there are two strings $j = 1, 2$, and their group velocity is simply given by [30,31,36]

$$v^{\rm eff}_{j,\lambda} = \frac{e'_j(\lambda)}{p'_j(\lambda)} = q_j \frac{e'_j(\lambda)}{2\pi\rho^T_{j,\lambda}}, \tag{9}$$

where e_j is the quasiparticle energy given by

$$e_j(\lambda) = 4JA_j(\lambda), \tag{10}$$

p_j is the quasiparticle momentum, and the total density of states $\rho^T_{j,\lambda} = \rho_{j,\lambda} + \rho^h_{j,\lambda}$ is given [58,64] by the Bethe equation (which is particularly simple since the model is noninteracting),

$$\rho^T_{j,\lambda} = q_j \frac{1}{N}\left[\sum_{k=1}^{N/2} A_j\left(\lambda + \frac{4}{\pi}\xi_{2k}\right) + \frac{N}{2}A_j(\lambda)\right], \tag{11}$$

for a system of size N, with the function $A_j(\lambda)$ defined as

$$A_j(\lambda) = \frac{\pi}{4}\frac{q_j}{\cosh(\pi\lambda/2)}. \tag{12}$$

In these equations, $q_1 = 1, q_2 = -1$. In the interacting case, all of these quantities would be "dressed" and would become a functional of the quasiparticle densities ρ_j.

As expected, since the model is noninteracting, the group velocity does not depend on the density ρ of the other quasiparticles. However, it does depend on the inhomogeneous variables ξ_i. It is thus clear that some kind of averaging over these random variables needs to be done in order to formulate a hydrodynamic theory of this random quantum spin chain.

B. Averaging and coarse graining

In order to average the random variables ξ_i, we go back to the physical picture of hydrodynamics and divide the system into mesoscopic hydrodynamic cells large enough to be in the thermodynamic limit. Let the system length be L and let it be divided in $N \gg 1$ subcells of size $\Delta x = L/N \gg a$, with a the lattice spacing. For a given disorder realization, the velocity in each hydrodynamic cell is given by (9). These velocities depend on our choice of subcell division, but as we will see this dependence drops out of the final result.

Given these velocities, we can easily construct the trajectory of a given quasiparticle from its initial position $x = 0$. Let us find the time required for a quasiparticle of type j with rapidity λ, initially at $x = 0$, to reach $x = M\Delta x$. It is given by [65]

$$t_x = \Delta x \sum_{i=1}^{M} \frac{1}{v_i}, \tag{13}$$

with v_i the velocity of the ith cell. We then have, using (9),

$$t_x = \Delta x \frac{2\pi}{e'} \sum_{i=1}^{M} \rho_i^T. \tag{14}$$

Since ρ^T is a sum of random variables, we can use the central limit theorem to deduce that both ρ^T and t_x are Gaussian distributed (provided the hydrodynamic cells are large enough, and $M \gg 1$). This also shows that the result is largely independent of the distribution chosen for the random parameter ξ, as long as the central limit theorem is applicable, as is the case for the distributions considered in this paper.

Thus we have following result: the time taken for a quasiparticle to move over a distance x is Gaussian distributed, with the average time being given by

$$\overline{t_x} = x\frac{2\pi\overline{\rho^T}}{e'}, \tag{15}$$

where $\overline{\rho^T}$ is the disorder average of ρ^T. This quantity is clearly independent from our choice of hydrodynamic cells—it only depends on x, not M, or Δx. The standard deviation reads

$$\sigma[t_x] = \sqrt{\frac{\Delta x}{2N_{\rm sub}}}\sqrt{x}\frac{2\pi\sigma\left[A\left(\lambda + \frac{2}{\eta}\xi\right)\right]}{e'},$$

where $N_{\rm sub}$ is the number of lattice sites inside a cell and $\sigma[A(\lambda + \frac{2}{\eta}\xi)]$ is the standard deviation of the function defined in Eq. (12). Note that $\sqrt{\frac{\Delta x}{2N_{\rm sub}}} = \sqrt{\frac{a}{2}}$ with a the lattice spacing, implying that the standard deviation of t_x is also independent of our choice of hydrodynamic cells. Thus we conclude that the distribution of t_x does not depend on the partition of hydrodynamic cells and is well defined.

We define the average velocity $v^\star$ via the relation $v^\star\overline{t_x} = x$. This yields

$$v^\star = \frac{e'}{2\pi\overline{\rho^T}} = \overline{(v^{\rm eff})^{-1}}^{-1}. \tag{16}$$

Note that this is *not* the average of $v^{\rm eff}$ over disorder.

The probability distribution of the time it took for the quasiparticle to move over a distance x thus reads

$$P_x(t) = \frac{1}{\sqrt{2\pi\Gamma x}} e^{-(t-x/v^\star)^2/2\Gamma x}, \tag{17}$$

$$\Gamma(\lambda) \equiv \left\{ \frac{2\pi\sigma\left[A\left(\lambda + \frac{2}{\eta}\xi\right)\right]}{e'} \right\}^2 \frac{a}{2}. \tag{18}$$

This process is called *temporal diffusion* [66,67], as it looks like an usual diffusion process where the roles of space and time are exchanged. However, in the hydrodynamic limit, the spreading of the distribution is confined to region $(x/v^\star - t)^2 = O(\Gamma x)$ or $x = v^\star t[1 + O(\sqrt{\frac{\Gamma v^\star}{t}})]$. Thus, in the limit $\frac{\Gamma v^\star}{t} \ll 1$, we can replace x by $v^\star t$ and get

$$P(x,t) \approx \frac{1}{\sqrt{2\pi\Gamma(v^\star)^3 t}} e^{-(x-v^\star t)^2/2\Gamma(v^\star)^3 t}, \tag{19}$$

which corresponds to a biased random walk. A similar temporal diffusion equation recently appeared in the context of energy transport in a random conformal field theory [67]. In all the numerical results below, we have checked that the difference between the temporal and ordinary diffusion descriptions is negligible in the hydrodynamic limit.

For generic initial condition of the quasiparticles, $\rho^0(x, t = 0)$, the evolution should thus read

$$\rho(x,t) = \int \frac{1}{\sqrt{4\pi Dt}} e^{-(x-x_0-v^\star t)^2/4Dt} \rho^0(x^0) dx^0, \tag{20}$$

with $D = \Gamma(v^\star)^3/2$ since the quasiparticles are noninteracting. Reintroducing the string and rapidity labels, we find that the quasiparticle density satisfies the following hydrodynamic equation:

$$\partial_t \rho_{j,\lambda}(x,t) + v^\star_{j,\lambda} \partial_x \rho_{j,\lambda}(x,t) = D_{j,\lambda} \partial_x^2 \rho_{j,\lambda}(x,t), \tag{21}$$

where $D_{j,\lambda} \equiv \frac{\Gamma_{j,\lambda}(v^\star_{j,\lambda})^3}{2}$ is a diffusion constant due to the disorder. We emphasize that the transport coefficients $v^\star$ and D in this equation *do not* depend on the details of our coarse-graining procedure—in particular, they do not depend on the size of the hydrodynamic cells Δx as long as $L \gg \Delta x \gg a$. We emphasize that contrary to diffusive corrections due to thermal fluctuations, the diffusive term in the above equation is diagonal in the quasiparticle basis and occurs even in the noninteracting case; in the interacting case, the off-diagonal terms are nonzero due to scattering between different quasiparticle species. For interacting random chains, we expect the argument above to carry over for the average velocity (16), but the diffusion matrix should be more complicated as it will have contributions from interactions and disorder. We leave a detailed analysis of the interacting case for future work.

IV. NONEQUILIBRIUM TRANSPORT

We now use the hydrodynamic equation derived above to study nonequilibrium energy and spin transport in the random spin chain (5). This will also allow us to benchmark and test the validity of the hydrodynamic approach and investigate the importance of the diffusive terms due to disorder. The energy and spin densities can be expressed in terms of the quasiparticle densities as

$$\epsilon(x,t) = \sum_j \int \rho_{j,\lambda}(x,t) e_j(\lambda)\, d\lambda, \tag{22}$$

$$s_z(x,t) = \frac{1}{2} - \sum_j n_j \int \rho_{j,\lambda}(x,t)\, d\lambda, \tag{23}$$

where n_j is given, in our case, by $n_1 = n_2 = 1$.

A. Energy transport

We first discuss energy transport. We consider a lattice of $L = 200$ sites prepared in a thermal state with $\beta = 1$, but with an interval of 32 sites in the middle of the system prepared in an infinite-temperature state ($\beta = 0$). The time evolution of the energy density profile can then be straightforwardly extracted from the free-fermion representation (6). We note that due to next-to-nearest interactions, we have to define energy density on two sites instead of one. We also emphasize that since the initial condition has a mirror symmetry about the middle of the lattice, one expects the evolution to be symmetric as well. However, this is only guaranteed if the sample of random variables ξ_i is symmetric about $\xi = 0$—this is due to the presence of imaginary interaction in Hamiltonian (6) which breaks this mirror symmetry. To retain the mirror symmetry exactly in the numerical data, we have ensured that the samples taken for the random variables are symmetric.

We then compare the numerical results from the solution of the hydrodynamic equation (21), combined with formula (22). Figure 1 show the hydrodynamic prediction for the energy density (solid line) compared to lattice data, for different disorder strengths $W = 0$ (clean case), $W = 0.6$, and $W = 2.0$. We also show the ballistic hydrodynamic prediction ignoring diffusive corrections (dashed line)—formally setting $D = 0$ in the hydrodynamic equation. The agreement between the numerics and hydrodynamics is excellent, and we find that diffusive corrections are needed to accurately describe the numerical data, especially at stronger disorder.

B. Spin transport

We also consider spin transport starting from an initial domain-wall state $|\psi_0\rangle = |\uparrow\uparrow \ldots \uparrow\downarrow \ldots \downarrow\downarrow\rangle$ (see Ref. [43] and references therein). This initial state has been considered for clean XXZ spin chains in several recent works: it leads to a steady state with zero entropy, where diffusive terms due to interactions and thermal fluctuations are expected to vanish. The hydrodynamic predictions for the local magnetization and numerical data are compared in Fig. 2. Here, also, Eq. (21) provides an excellent description of the numerics and our data clearly show the presence of diffusion in this noninteracting setting where no thermal fluctuations are present [68]. We expect this initial state to also be useful to extend our approach to interacting random spin chains, as it would allow one to isolate diffusive terms due to disorder (since the diffusion matrix coming from interactions vanishes). Comparing the predictions from hydrodynamics to numerical results in the interacting case would, however, be very numerically

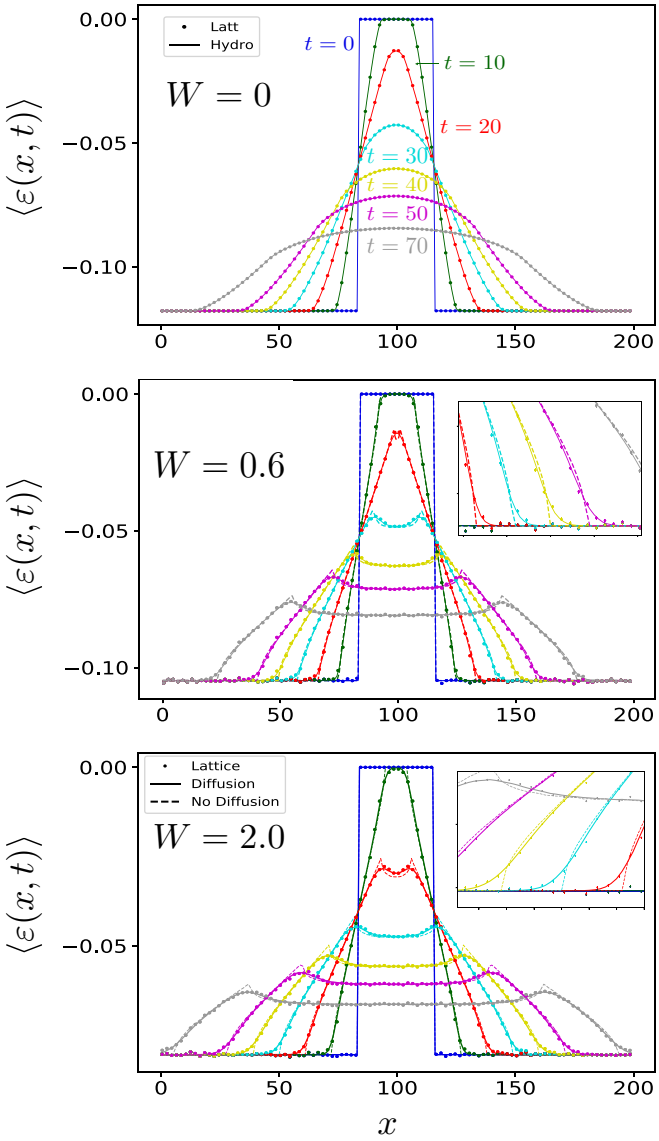

FIG. 1. Nonequilibrium energy transport. The different panels show the evolution of the energy density as a function of time for different disorder strengths, for an initial state at temperature $T = 1$ with a small region of the system locally at infinite temperature. We compare exact numerical results and the hydrodynamic prediction from the solution of Eq. (21), with and without the diffusive term. As disorder is increased, the diffusive effects become more pronounced and diffusive corrections are needed to reproduce the numerical data. The numerical data were averaged over $\sim 3 \times 10^3$ and $\sim 1.6 \times 10^4$ disorder realizations for $W = 0.6$ and $W = 2.0$, respectively.

demanding because of the average over disorder, and is left for future work.

V. PROPERTIES OF LOW-ENERGY QUASIPARTICLES

So far, our discussion has focused on macroscopic energy and spin transport, which is dominated by fast quasiparticles. In addition to these typical, fast quasiparticles, however, these models also have slow quasiparticles at energy $|E| \approx 0$. These are important, e.g., for low-temperature transport, as well as for the behavior of local autocorrelation functions

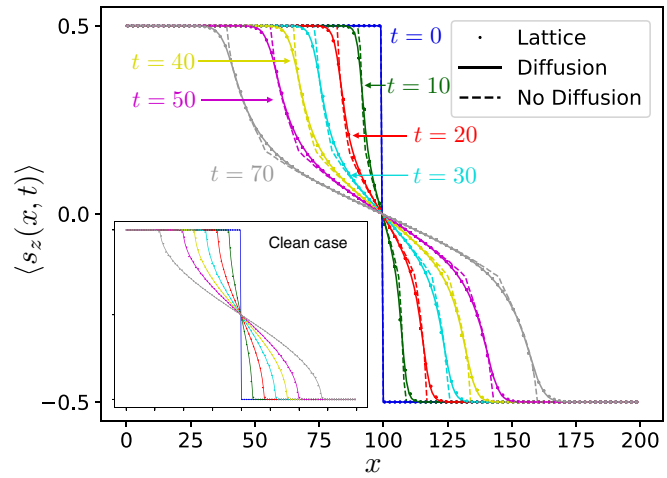

FIG. 2. Spin domain-wall initial state. Comparison of the hydrodynamic prediction (21) with numerical results for a spin domain-wall initial state. The disorder strength is $W = 0.6$ and numerical results are averaged over $\sim 2 \times 10^3$ disorder realizations. The hydrodynamic equation including diffusive terms (solid line) describes the numerical results much more accurately than the purely ballistic prediction (dashed line). This establishes the presence of diffusive terms in the hydrodynamic description of this noninteracting system, even for an initial state that does not incorporate thermal fluctuations.

at late times. We discuss the nature of these quasiparticles here. We first explore the properties of wave functions, both numerically and analytically, and find that these undergo a quasilocalization transition for the exponential disorder distribution (4). We then apply the thermodynamic Bethe-ansatz results in Sec. III to study the asymptotic behavior of the velocity and density of states as $|E| \to 0$. Our discussion here is confined to the noninteracting model (5).

A. Spatial correlations of eigenstates

We first discuss the properties of single-particle eigenstates. Because of the Bethe-ansatz integrability of the model, eigenstates are never localized in the conventional sense and most are completely delocalized [58]. However, the states closest in energy to zero have anomalous properties, which show up in the hydrodynamic framework as very slow velocities. We now address these properties more directly. Figure 3 shows that the inverse participation ratio (IPR) $\sum_x |\psi_x|^4$ rises steeply for states very near zero energy; thus, these are less spread out than the rest of the spectrum, which is fully delocalized. In the rest of this section, we will focus on the few relatively localized states near zero energy.

Given the anomalously large IPRs of states near zero energy, it is natural to investigate their spatial structure. It turns out this structure is simple and striking. The upper panel of Fig. 4 plots the spatial profile of each eigenstate against the eigenstate index. States near $|E| = 0$ are halfway up the y axis; they are evidently strongly peaked at certain lattice sites and the peak locations are the *same* for each such state. In other words, these states exhibit a very strong form of Chalker scaling [69,70]. Further, the peak locations and intensities follow a simple pattern (lower panel of Fig. 4): the amplitude of each peak is $\propto \cosh(\xi_j)$, where ξ_j is the

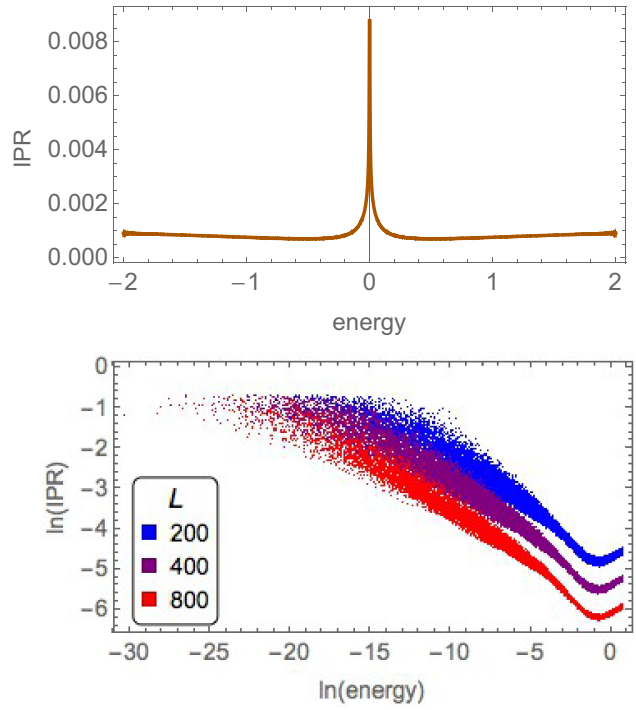

FIG. 3. Low-energy wave functions. Upper panel: IPR vs energy for the noninteracting model (5) with Gaussian-distributed disorder with parameters $W = 1$, $L = 2000$ (single, typical realization). Lower panel: Log-log plot of IPR vs energy for an exponential disorder distribution, with $\phi = 0.5$, binned over 500 realizations for each system size.

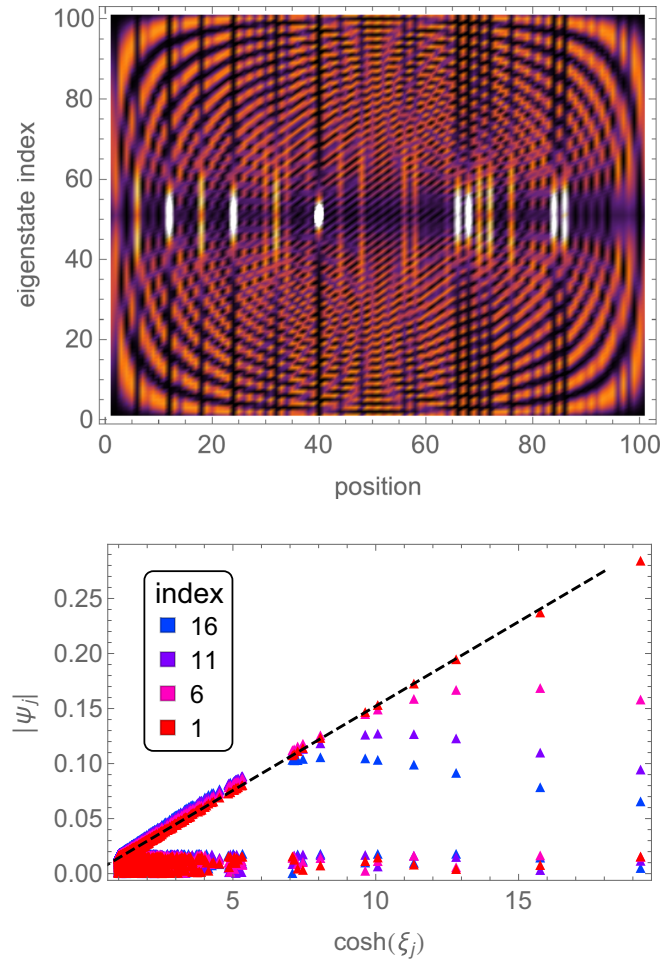

FIG. 4. Spatial structure of low-energy wave functions. Upper panel: density plot of eigenstate probability density in space for a single eigenstate in a single realization at $L = 100$; y axis is the eigenstate index, a proxy for the energy. All the states near zero energy are concentrated at the same sites, i.e., they are perfectly spatially correlated. Lower panel: scatterplot of eigenstate amplitude vs inverse hopping matrix element $\cosh(\xi_j)$ for the anomalous eigenstates for $L = 2000$. The figure shows four eigenstates; states with the smallest $|E|$ are shaded red, while those with larger $|E|$ are shaded blue.

nearest-neighbor hopping at the peak. These observations can be qualitatively understood in terms of a simple picture in which each eigenstate carries some nonzero current, which (since the eigenstate is time invariant) must be the same at every link. Since the tunneling rates vary drastically from one link to the next, this uniform current is maintained by having the density pile up near weak links. As one moves away from zero energy, the states lose intensity first at the strongest maxima (Fig. 4); higher-energy wave functions bypass these weak links instead of piling up near them.

We find, numerically, that these anomalous states are supported entirely on even sites (i.e., sites for which the next-nearest neighbor coupling is absent). This is intuitively plausible since no value of ξ_j can simultaneously suppress both the nearest-neighbor and next-nearest-neighbor hopping out of an odd site.

B. Multifractality and quasilocalization

The eigenfunctions near zero energy are sharply peaked at a few (even) sites, suggesting that they might be critical rather than conventionally delocalized. The nature of these states is highly sensitive to the tails of the disorder distribution. So far we have considered Gaussian distributions of the ξ_j; numerical extraction of the IPR at the accessible system sizes does not settle whether the wave functions are localized or critical. However, the relationship between the wave-function amplitudes and $\cosh(\xi_j)$ allows us to address this question semianalytically. Among L Gaussian random variables, the largest value is likely to be $\exp(-\xi^2/W^2) \simeq 1/L$, so $\xi = W\sqrt{\log L}$. The (unnormalized) wave-function amplitude at this site is therefore $\cosh(W\sqrt{\log L}) \sim \exp(W\sqrt{\log L})$. Meanwhile, the typical value of $\cosh(\xi_j)$ is of the order of unity, and occurs $O(L)$ times. Thus the weakest link in a typical sample does not affect its properties overall. We therefore expect that the low-energy wave functions in the Gaussian case are asymptotically not multifractal.

This reasoning also suggests that to get multifractal wave functions, it suffices to change the disorder distribution from Gaussian to exponential, $P(\xi) \propto \exp(-\phi|\xi|)$. In this case, repeating the argument in the previous paragraph gives that the largest typical peak has amplitude $L^{1/\phi}$. When $\phi < 2$, the wave function piles up at the weakest link and is "quasilocalized" in the sense that its IPR is independent of system size. Numerical simulations clearly show this quasilocalized behavior at small ϕ, as well as the expected multifractal

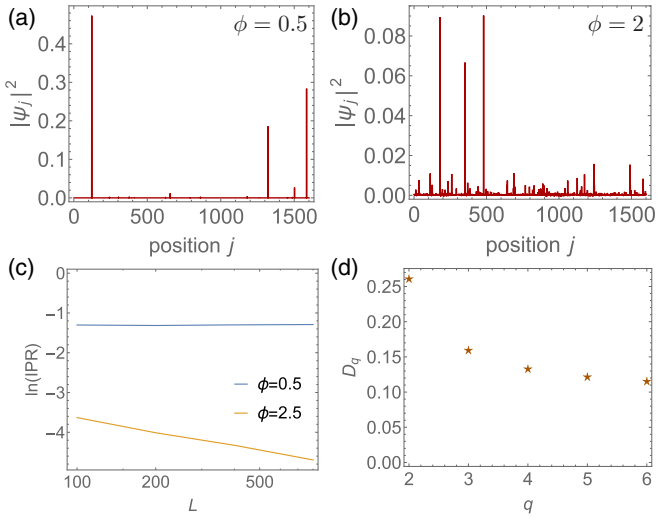

FIG. 5. Properties of the noninteracting model with an exponential distribution of ξ_j. (a),(b) Spatial structure of single low-energy eigenstates for $\phi = 0.5$ (quasilocalized) and $\phi = 2$ (multifractal), for system size $L = 2000$. (c) Decay of the IPR with system size in the two phases, averaged over 1000 samples at each size. (d) Multifractal exponent D_q (where q labels moments of the wave function) for $\phi = 2$. The exponents are extracted for system sizes from $L = 100$ to $L = 800$ with 1000 samples per size. For conventional delocalized states, such as the states away from zero energy, one would have $D_q = 1$ for all q.

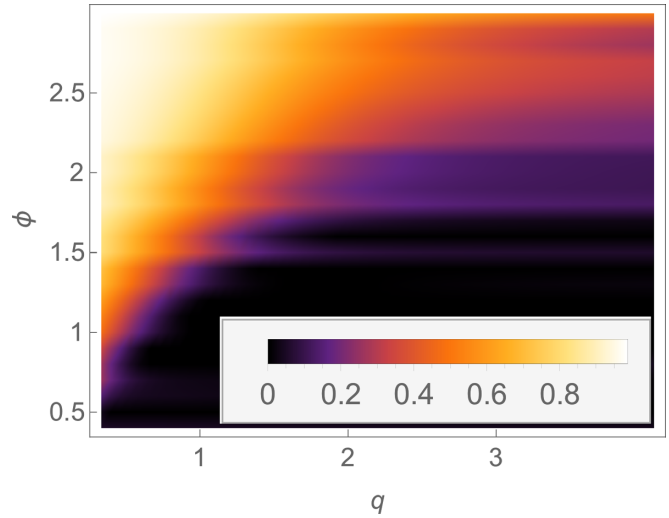

FIG. 6. Multifractal spectrum. Density plot of the quantity D_q as a function of q and the inverse disorder strength ϕ for an exponential distribution. The region in black for $\phi < 2$ is quasilocalized.

behavior at larger ϕ [Fig. 5(d)]. We characterize multifractality through the quantity [71]

$$D_q = \frac{1}{(1-q)\log L}\overline{\log \sum_x |\psi_x|^{2q}}, \tag{24}$$

where $\overline{O}$ refers to the disorder average of the quantity O. For each sample, we take the lowest-$|E|$ state.

In the quasilocalized regime, $D_q = 0$ for $q > 1$. Strictly speaking, this statement is asymptotically true in the following sense: wave functions at any fixed energy away from zero are delocalized, but as one approaches zero energy, their IPR approaches a fixed, size-independent value (Fig. 3). Thus, there is no mobility edge. Although the IPR is finite, unlike an Anderson insulator, the quasilocalized phase has $D_q > 0$ for $q < 1$: although the wave function has a finite fraction of its weight concentrated in a few peaks, the rest of the weight is spread out evenly rather than falling off exponentially away from the peaks (Fig. 6). Finally, we remark that although its IPR is independent of system size, this does not imply that a particular state will be unaffected by adding sites to one end of the system: the wave function will remain very sharply peaked at the weakest link, but the location of this link will move as sites are added to the system.

C. GHD approach to quasilocalization

We now use the results in Sec. III to consider the behavior of quasiparticles in the $|E| \to 0$ limit. From Eq. (10), we see that these quasiparticles correspond to large $|\lambda|$: in fact, $e_j(\lambda) \sim e^{-\pi|\lambda|/2}$. In what follows, we suppress the index j and denote the energy as E. The limiting behavior of the velocity and the density of states is sensitive to the tails of the disorder distribution. For the sample-averaged density of states, Eq. (11) yields

$$\rho^T_{1,\lambda} = \left\langle \frac{\pi}{8\cosh(\pi\lambda/2 + 2\xi)} \right\rangle_{\text{dis}} + \frac{\pi}{8\cosh(\pi\lambda/2)}, \tag{25}$$

where $\langle\cdot\rangle_{\text{dis}}$ denotes the average over disorder. If the disorder is bounded or falls off faster than exponentially, one can safely approximate $\cosh(x) \approx e^x/2$ for large enough λ. The quasiparticle velocity [given by Eq. (9)] therefore remains nonzero in the $\lambda \to \infty$ limit, so transport is asymptotically ballistic (but with a slower velocity). Likewise, the density of states remains finite. To find the density of states, one notes that the number of states in a rapidity interval $\delta\lambda$ is given by $\rho^T_{1,\lambda}\delta\lambda$. These cover an energy window $\delta E = E'(\lambda)\delta\lambda = e^{-\pi\lambda/2}\delta\lambda$. Thus, $\rho(E) = \rho^T_{1,\lambda}/E'(\lambda)$, which remains finite for Gaussian-distributed disorder in the $|\lambda| \to \infty$ limit (although, in practice, the suppression is quantitatively quite large).

However, for distributions $P(\xi)$ with exponential or slower tails, computing the expectation value (25) is more subtle. We focus on the exponential case $P(\xi) = \frac{1}{2\phi}\exp(-\phi|\xi|)$, which was discussed numerically above. In this case, the expectation value (25) reads

$$\frac{\phi\pi}{4}\int_{-\infty}^{\infty} d\xi \frac{e^{-\phi|\xi|}}{\cosh(\pi\lambda/2 + 2\xi)}. \tag{26}$$

To get compact expressions for the asymptotics, we approximate $\cosh(\pi\lambda/2 + 2\xi) \approx \frac{1}{2}e^{|\pi\lambda/2+2\xi|}$. There are two cases. When $\phi > 2$, the integral is dominated by small $|\xi|$ and we get

$$\left\langle \frac{\pi}{8\cosh(\pi\lambda/2 + 2\xi)} \right\rangle_{\text{dis}} \approx \frac{\phi\pi e^{-\pi\lambda/2}}{2(\phi-2)}(1 - e^{-(\phi-2)\pi\lambda/2}) + \cdots, \tag{27}$$

where $\cdots$ indicates terms that do not become singular in the limit $\phi \to 2$. Thus the zero-energy density of states and

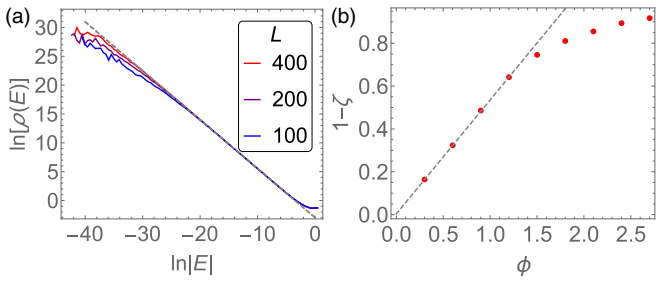

FIG. 7. Density of states and quasilocalization. (a) Log-log plot of density of states for various system sizes, in the case where ξ_k are distributed exponentially with the parameter $\phi = 0.3$. The density of states diverges as $|E|^{-\zeta}$ at low energies. (b) Exponent $1-\zeta$ vs ϕ. For small ϕ, we find a good linear fit to $\zeta = 1 - 0.53\phi$, which is in reasonable agreement with the Bethe-ansatz prediction $\zeta = 1 - \phi/2$ (see main text).

velocity remain finite when $\phi > 2$, but respectively diverge and vanish as $\phi \to 2^+$. Note that there are nonanalytic corrections to the density of states, even in this regime: specifically, $|\rho(E) - \rho(0)| \sim E^{\phi-2}$.

In the opposite limit $\phi < 2$, Eq. (25) is dominated by $|\xi| \approx \pi\lambda/4$. In this case, we have instead

$$\left\langle \frac{1}{\cosh(\pi\lambda/2 + 2\xi)} \right\rangle_{\text{dis}} \sim e^{-\phi\pi\lambda/4}. \tag{28}$$

The velocity then vanishes as $v(\lambda) \sim \exp[-(\pi\lambda/2)(1 - \phi/2)]$ or, equivalently, $v(E) \sim |E|^{1-\phi/2}$. Correspondingly, the density of states $\rho(E)$ diverges as

$$\rho(E) \sim |E|^{-1+\phi/2}. \tag{29}$$

This behavior of the density of states is borne out numerically (Fig. 7).

Thus, the dispersion relation of elementary excitations within generalized hydrodynamics agrees with our simple counting estimate in Sec. V: a transition occurs when $\phi = 2$. When $\phi > 2$, the velocity approaches a finite value as $|E| \to 0$, so quantities such as the local autocorrelation function behave in an asymptotically ballistic fashion. On the other hand, when $\phi < 2$, the velocity vanishes as $|E| \to 0$ and the local autocorrelation function will, in general, be anomalous. It is interesting to note that despite the very local character of the rare low-energy states due to almost disconnected sites, they appear naturally as slow quasiparticles in the hydrodynamics framework.

VI. OPERATOR SPREADING AND LOCAL AUTOCORRELATIONS

A. Front broadening

We close this paper by discussing the consequences of our results for operator spreading in random integrable systems. The dynamics of operator spreading has attracted a lot of attention in recent years due to its possible connection to many-body quantum chaos [72–87]. Under unitary dynamics, initially local operators spread in space ballistically (unless the system is many-body localized), with an operator "front" or light cone that generically broadens diffusively as $t^{1/2}$ in one-dimensional chaotic (nonintegrable) quantum systems. This is in sharp contrast to (clean) noninteracting systems that have an operator front that broadens as $t^{1/3}$ [55], governed by an Airy kernel. However, *interacting* integrable systems have been argued to have a front that also broadens as $t^{1/2}$ [51,88], just like chaotic systems (with the notable exception of nongeneric zero-entropy initial states such as the spin domain-wall initial state discussed above [68]). In integrable systems, the operator front is governed by the fastest quasiparticle in the system [51]: from our hydrodynamic description of random integrable spin chains, it is natural to expect this front to broaden diffusively even in the noninteracting case since the fastest quasiparticle follows a biased random walk. For these systems, the diffusive broadening of the operator front is due to the local disorder which causes the fastest quasiparticle (on average) to "wiggle" around its average trajectory.

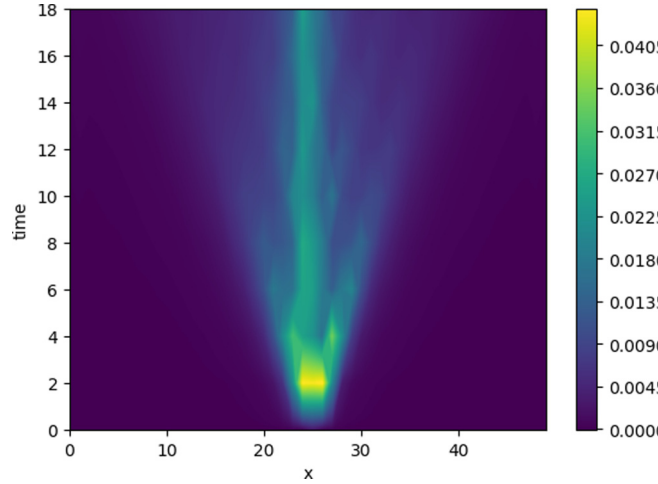

FIG. 8. Operator spreading. Contour plot of the OTOC $C(x,t) = \frac{1}{2}\langle[n_x(t), n_0(0)]^2\rangle$ for disorder strength $W = 1$ and temperature $T = 1$, averaged over 100 realizations. The ballistic spreading of operators with time is clearly visible, as well as quasilocalized quasiparticles due to the anomalous low-energy properties of this model.

In order to characterize operator spreading in our system, we compute a specific out-of-time ordered commutator (OTOC) [72–74] given by $C(x,t) = \frac{1}{2}\langle[n_x(t), n_0(0)]^2\rangle$ in a given thermal state, with $n_x = c_x^\dagger c_x$ the particle density in the fermionic language. Figure 8 shows $C(x,t)$ averaged over 100 disorder realizations for $W = 1$ and temperature $T = 1$, where a clear ballistic light cone can be observed. We also remark that the OTOC shows significant weight that remains near $x = 0$ even after a long time. This behavior has to do with the anomalous low-energy states (Sec. V) and we will return to it below.

We now focus on the operator front (light cone) and investigate whether it broadens as $t^{1/3}$, as expected for clean noninteracting systems, or as $t^{1/2}$, due to diffusive effects. We start with the clean case (XX model) and show scaling collapses of the OTOC near the front. It is clear from Fig. 9 that the data collapse almost perfectly using a $t^{1/3}$ ansatz. This is consistent with expectations in the clean case, where the OTOC shows oscillations characteristic of an Airy kernel associated with these higher-order corrections to hydrodynamics [55]. In the random case, we expect that these oscillations should vanish

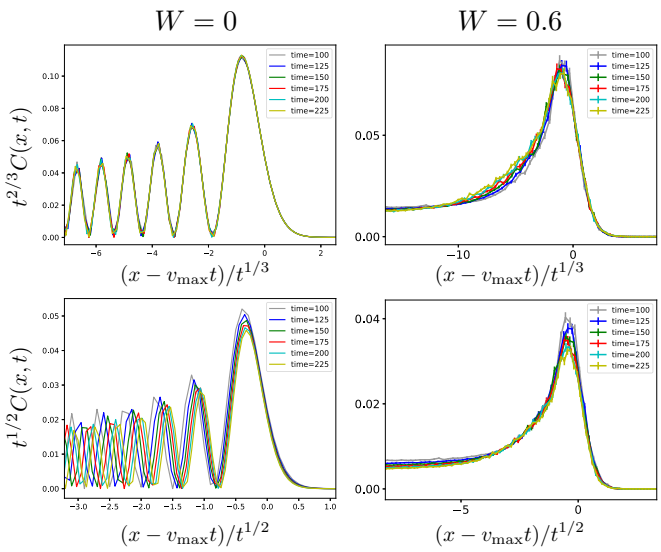

FIG. 9. Scaling of the operator front. Scaling collapses of the OTOC near the operator front. Left panel: For the clean case, the front has oscillations as expected from an Airy kernel. The scaling with exponent 1/3 (upper left) leads to a better collapse than the diffusive scaling 1/2 (lower left). Right panel: Similar collapses for the random case are inconclusive.

and that the front will collapse onto a diffusive form. From Fig. 9, it is clear that there are no characteristic oscillations near the front. However, scaling our data with both $t^{1/2}$ and $t^{1/3}$ leads to equally good collapses and suggests that such collapses are not a very conclusive way to measure the exponent α of the front broadening t^{α}. We also considered collapses from the time evolution following local quenches, with very similar results. Nevertheless, our transport results combined with our hydrodynamic theory strongly suggest that $\alpha = 1/2$ even for random noninteracting chains.

B. Slow local relaxation

We now turn briefly to the part of the local operator that remains near its initial position at late times. Since we are considering a noninteracting model, we can equivalently consider the return probability of an initially local wave packet [89]. We should distinguish between average and typical behavior: *typically*, the initial site is not a weak link, so anomalous wave functions have no support there. However, the site-averaged local autocorrelation function does receive a contribution from rare sites. Once again, we discuss this for the exponential distribution (4) in the quasilocalized phase, $\phi < 2$.

We consider the probability that a particle initially localized at site x has moved a distance less than one lattice site at time t. This quantity is proportional to the (mean) local autocorrelation function $C_0(t) = \overline{\langle S_i^z(t) S_i^z(0)\rangle}$. We focus on i even and infinite temperature. In generalized hydrodynamics, this can be expressed as

$$C_0(t) \sim \sum_{j=1,2} \int d\lambda \langle \rho(\lambda) m_j(\lambda)^2 \Theta(a - |v(\lambda)t|)\rangle_{\rm dis}, \qquad (30)$$

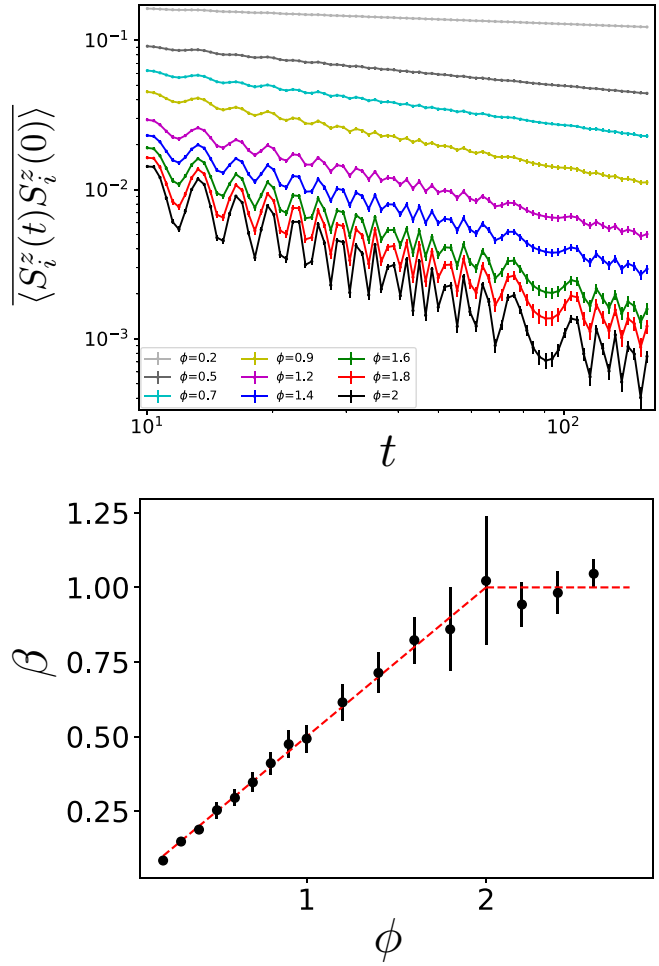

FIG. 10. Anomalous local relaxation. Top panel: Algebraic decay of the average local structure factor $C_0(t)$ as a function of time, for various disorder strengths ϕ. This power-law decay for small values of ϕ can be observed up to very long times. Bottom panel: Decay exponent of the average local correlation function $C_0(t)$, as a function of disorder strength ϕ. We find that $C_0(t) \sim t^{-\beta}$, where $\beta \approx \phi/2$ throughout the quasilocalized phase $\phi < 2$. The generalized hydrodynamics prediction $\beta = \phi/2$ is indicated by a dashed red line. When $\phi > 2$, one has conventional ballistic behavior, $C_0(t) \sim 1/t$.

where at infinite temperature for a free-fermion model, $\rho^T \sim \rho$, $a = 1$ is the lattice spacing, and $m_j(\lambda) = n_j = 1$ is the spin of the quasiparticles. Focusing on low-energy quasiparticles, this integral can be written out as

$$C_0(t) \sim \int d\lambda\, d\xi\, e^{-\phi|\xi|} \rho^T(\lambda, \xi) \Theta[1 - |v(\lambda, \xi)t|]. \qquad (31)$$

We now resolve the step function and approximate $\rho_t(\lambda, \xi) \simeq e^{-\pi\lambda/2 + 2\xi} \Theta(\lambda - 4\xi/\pi)$, as in Sec. V C, to rewrite this expression in terms of the double integral,

$$C_0(t) \sim \int_{\frac{1}{2}\log t}^{\infty} d\xi \int_{4\xi/\pi}^{\infty} d\lambda e^{-\pi\lambda/2} e^{(2-\phi)\xi} \sim t^{-\phi/2}. \qquad (32)$$

Higher-energy quasiparticles give rise to a ballistic decay $1/t$ that is subleading when $\phi < 2$. Thus, throughout the quasilocalized phase, the autocorrelation function decays slower than one would expect for a model with ballistic transport.

Numerical simulations of the autocorrelation function give results in very good agreement with this exponent (Fig. 10). We emphasize that in the argument above, it was crucial to disorder average the full autocorrelation function—separately averaging the velocity and the density of states would yield an incorrect exponent $\phi/(2-\phi)$, in clear disagreement with our numerical results. The local velocity is inversely proportional to the local density of states and capturing these correlations is essential to deriving the correct anomalous exponent.

We will show elsewhere that anomalous decay of local autocorrelation functions occurs in other models such as XXZ as well; however, the possibility of *subdiffusive* behavior is specific to the disordered noninteracting models, as generic interacting models will have a finite diffusion constant due to interactions.

VII. DISCUSSION

We studied the nonequilibrium dynamics of integrable spin chains with correlated disorder that preserves integrability. Focusing on the noninteracting case, we formulated a (generalized) hydrodynamic theory for such random systems and described the emergence of diffusive corrections due to quasiparticles scattering off random impurities. This provides a mechanism for diffusion that is different from the recent theories of diffusive corrections to GHD in *clean* integrable quantum systems. The predictions from hydrodynamics were compared to numerical results obtained from exact diagonalization of the free-fermion problem. Both spin and energy transport can be described very accurately using hydrodynamics, provided diffusive corrections are included. Moreover, we have shown that low-energy quasiparticles are very sensitive to the tails of the disorder distribution and can become quasilocalized, leading to an anomalous decay of local autocorrelation functions.

We expect our results to generalize naturally to all *interacting* random integrable systems [56–58]. In general, we expect a complicated interplay between diffusive corrections due to disorder and due to thermal fluctuations and interactions. However, a simpler intermediate setup would be to consider initial states for which thermal fluctuations vanish, such as the spin domain-wall initial state considered above. For such initial states, we expect our predictions to extend naturally to the interacting case, and it would be interesting to compare the hydrodynamic predictions to matrix product state simulations.

Our results also indicate that diffusive broadening of the operator front can occur even in some noninteracting systems, which are clearly nonchaotic. These models could be used as a testbed for future diagnostic tools to distinguish chaotic from integrable systems. These models are also natural from the point of view of integrability breaking: adding integrability-breaking perturbations to a random integrable chain at strong disorder could lead to either thermalization or to many-body localization. The results of Ref. [58] suggest that the regime of ballistic transport escaping localization might not be as fine tuned as one could have expected, and it would be interesting to investigate whether hydrodynamics can still accurately describe transport away from the integrable limit.

ACKNOWLEDGMENTS

We thank Vir Bulchandani and Fabian Essler for useful comments on this manuscript. This work was supported by the US Department of Energy, Office of Science, Basic Energy Sciences, under Award No. DE-SC0019168 (U.A. and R.V.), and by NSF Grant No. DMR-1653271 (S.G.). Most numerical simulations were performed at the Massachusetts Green High Performance Computing Center (MGHPCC).

[1] I. Bloch, J. Dalibard, and W. Zwerger, Rev. Mod. Phys. **80**, 885 (2008).
[2] T. Kinoshita, T. Wenger, and D. S. Weiss, Nature (London) **440**, 900 (2006).
[3] T. Langen, S. Erne, R. Geiger, B. Rauer, T. Schweigler, M. Kuhnert, W. Rohringer, I. E. Mazets, T. Gasenzer, and J. Schmiedmayer, Science **348**, 207 (2015).
[4] D. Leibfried, R. Blatt, C. Monroe, and D. Wineland, Rev. Mod. Phys. **75**, 281 (2003).
[5] L.-M. Duan and C. Monroe, Rev. Mod. Phys. **82**, 1209 (2010).
[6] R. Blatt and C. F. Roos, Nat. Phys. **8**, 277 (2012).
[7] M. W. Doherty, N. B. Manson, P. Delaney, F. Jelezko, J. Wrachtrup, and L. C. Hollenberg, Phys. Rep. **528**, 1 (2013).
[8] R. Schirhagl, K. Chang, M. Loretz, and C. L. Degen, Annu. Rev. Phys. Chem. **65**, 83 (2014).
[9] J. Kelly, R. Barends, A. G. Fowler, A. Megrant, E. Jeffrey, T. C. White, D. Sank, J. Y. Mutus, B. Campbell, Y. Chen, Z. Chen, B. Chiaro, A. Dunsworth, I.-C. Hoi, C. Neill, P. OMalley, C. Quintana, P. Roushan, A. Vainsencher, J. Wenner, A. N. Cleland, and J. M. Martinis, Nature (London) **519**, 66 (2015).
[10] R. Nandkishore and D. A. Huse, Annu. Rev. Condens. Matter Phys. **6**, 15 (2015).
[11] R. Vasseur and J. E. Moore, J. Stat. Mech. (2016) 064010.
[12] D. A. Abanin, E. Altman, I. Bloch, and M. Serbyn, arXiv:1804.11065.
[13] L. D'Alessio, Y. Kafri, A. Polkovnikov, and M. Rigol, Adv. Phys. **65**, 239 (2016).
[14] Y. Tang, W. Kao, K.-Y. Li, S. Seo, K. Mallayya, M. Rigol, S. Gopalakrishnan, and B. L. Lev, Phys. Rev. X **8**, 021030 (2018).
[15] P. Calabrese and J. Cardy, Phys. Rev. Lett. **96**, 136801 (2006).
[16] T. Prosen, Phys. Rev. Lett. **106**, 217206 (2011).
[17] J.-S. Caux and F. H. L. Essler, Phys. Rev. Lett. **110**, 257203 (2013).
[18] M. Fagotti and F. H. L. Essler, J. Stat. Mech. (2013) P07012.
[19] F. H. L. Essler and M. Fagotti, J. Stat. Mech. (2016) 064002.
[20] T. Prosen and E. Ilievski, Phys. Rev. Lett. **111**, 057203 (2013).
[21] B. Wouters, J. De Nardis, M. Brockmann, D. Fioretto, M. Rigol, and J.-S. Caux, Phys. Rev. Lett. **113**, 117202 (2014).
[22] E. Ilievski, M. Medenjak, and T. Prosen, Phys. Rev. Lett. **115**, 120601 (2015).

[23] E. Ilievski, J. De Nardis, B. Wouters, J.-S. Caux, F. H. L. Essler, and T. Prosen, Phys. Rev. Lett. **115**, 157201 (2015).

[24] E. Ilievski, M. Medenjak, T. Prosen, and L. Zadnik, J. Stat. Mech. (2016) 064008.

[25] M. Fagotti, M. Collura, F. H. L. Essler, and P. Calabrese, Phys. Rev. B **89**, 125101 (2014).

[26] M. Rigol, V. Dunjko, V. Yurovsky, and M. Olshanii, Phys. Rev. Lett. **98**, 050405 (2007).

[27] J.-S. Caux and R. M. Konik, Phys. Rev. Lett. **109**, 175301 (2012).

[28] M. Rigol, Phys. Rev. Lett. **103**, 100403 (2009).

[29] D. Bernard and B. Doyon, J. Stat. Mech. (2016) 064005.

[30] O. A. Castro-Alvaredo, B. Doyon, and T. Yoshimura, Phys. Rev. X **6**, 041065 (2016).

[31] B. Bertini, M. Collura, J. De Nardis, and M. Fagotti, Phys. Rev. Lett. **117**, 207201 (2016).

[32] G. El, Phys. Lett. A **311**, 374 (2003).

[33] G. A. El and A. M. Kamchatnov, Phys. Rev. Lett. **95**, 204101 (2005).

[34] V. B. Bulchandani, R. Vasseur, C. Karrasch, and J. E. Moore, Phys. Rev. B **97**, 045407 (2018).

[35] B. Doyon, T. Yoshimura, and J.-S. Caux, Phys. Rev. Lett. **120**, 045301 (2018).

[36] L. Bonnes, F. H. L. Essler, and A. M. Läuchli, Phys. Rev. Lett. **113**, 187203 (2014).

[37] V. B. Bulchandani, R. Vasseur, C. Karrasch, and J. E. Moore, Phys. Rev. Lett. **119**, 220604 (2017).

[38] B. Doyon, J. Dubail, R. Konik, and T. Yoshimura, Phys. Rev. Lett. **119**, 195301 (2017).

[39] L. Piroli, J. De Nardis, M. Collura, B. Bertini, and M. Fagotti, Phys. Rev. B **96**, 115124 (2017).

[40] E. Ilievski and J. De Nardis, Phys. Rev. Lett. **119**, 020602 (2017).

[41] B. Doyon and H. Spohn, SciPost Phys. **3**, 039 (2017).

[42] E. Ilievski and J. De Nardis, Phys. Rev. B **96**, 081118(R) (2017).

[43] M. Collura, A. De Luca, and J. Viti, Phys. Rev. B **97**, 081111(R) (2018).

[44] B. Doyon and T. Yoshimura, SciPost Phys. **2**, 014 (2017).

[45] X. Cao, V. B. Bulchandani, and J. E. Moore, Phys. Rev. Lett. **120**, 164101 (2018).

[46] J.-S. Caux, B. Doyon, J. Dubail, R. Konik, and T. Yoshimura, arXiv:1711.00873.

[47] B. Doyon, SciPost Phys. **5**, 054 (2018).

[48] V. Alba and P. Calabrese, Proc. Natl. Acad. Sci. USA **114**, 7947 (2017).

[49] J. Myers, M. J. Bhaseen, R. J. Harris, and B. Doyon, arXiv:1812.02082.

[50] J. De Nardis, D. Bernard, and B. Doyon, Phys. Rev. Lett. **121**, 160603 (2018).

[51] S. Gopalakrishnan, D. A. Huse, V. Khemani, and R. Vasseur, Phys. Rev. B **98**, 220303(R) (2018).

[52] J. De Nardis, D. Bernard, and B. Doyon, SciPost Phys. **6**, 049 (2019).

[53] S. Gopalakrishnan and R. Vasseur, Phys. Rev. Lett. **122**, 127202 (2019).

[54] H. Spohn, J. Math. Phys. **59**, 091402 (2018).

[55] M. Fagotti, Phys. Rev. B **96**, 220302(R) (2017).

[56] H. J. d. Vega and F. Woynarovich, J. Phys. A **25**, 4499 (1992).

[57] H. J. de Vega, L. Mezincescu, and R. I. Nepomechie, Phys. Rev. B **49**, 13223 (1994).

[58] F. H. L. Essler, R. v. d. Berg, and V. Gritsev, Phys. Rev. B **98**, 024203 (2018).

[59] R. Vosk and E. Altman, Phys. Rev. Lett. **110**, 067204 (2013).

[60] R. Vasseur, A. J. Friedman, S. A. Parameswaran, and A. C. Potter, Phys. Rev. B **93**, 134207 (2016).

[61] For a thorough review of TBA, we refer the interested reader to [64].

[62] C. N. Yang and C. P. Yang, J. Math. Phys. **10**, 1115 (1969).

[63] H. Spohn, *Large Scale Dynamics of Interacting Particles*, Theoretical and Mathematical Physics (Springer, Berlin, 2012).

[64] M. Takahashi, *Thermodynamics of One-Dimensional Solvable Models* (Cambridge University Press, Cambridge, 1999).

[65] We will momentarily omit the string number and rapidity/momentum subscripts to make the equations more readable.

[66] J. P. Boon, P. Grosfils, and J. F. Lutsko, Europhys. Lett. **63**, 186 (2003).

[67] E. Langmann and P. Moosavi, Phys. Rev. Lett. **122**, 020201 (2019).

[68] V. B. Bulchandani and C. Karrasch, Phys. Rev. B **99**, 121410(R) (2019).

[69] J. T. Chalker and G. J. Daniell, Phys. Rev. Lett. **61**, 593 (1988).

[70] J. Chalker, Physica A (Amsterdam) **167**, 253 (1990).

[71] F. Evers and A. D. Mirlin, Rev. Mod. Phys. **80**, 1355 (2008).

[72] A. Larkin and Y. N. Ovchinnikov, Sov. Phys. JETP **28**, 1200 (1969).

[73] S. H. Shenker and D. Stanford, J. High Energy Phys. 03 (2014) 067.

[74] J. Maldacena, S. H. Shenker, and D. Stanford, J. High Energy Phys. 08 (2016) 106.

[75] H. Liu and S. J. Suh, Phys. Rev. Lett. **112**, 011601 (2014).

[76] H. Casini, H. Liu, and M. Mezei, J. High Energy Phys. 07 (2016) 077.

[77] M. Mezei and D. Stanford, J. High Energy Phys. 05 (2017) 065.

[78] W. Brown and O. Fawzi, arXiv:1210.6644.

[79] A. Nahum, J. Ruhman, S. Vijay, and J. Haah, Phys. Rev. X **7**, 031016 (2017).

[80] A. Nahum, S. Vijay, and J. Haah, Phys. Rev. X **8**, 021014 (2018).

[81] C. W. von Keyserlingk, T. Rakovszky, F. Pollmann, and S. L. Sondhi, Phys. Rev. X **8**, 021013 (2018).

[82] V. Khemani, A. Vishwanath, and D. A. Huse, Phys. Rev. X **8**, 031057 (2018).

[83] T. Rakovszky, F. Pollmann, and C. W. von Keyserlingk, Phys. Rev. X **8**, 031058 (2018).

[84] A. Chan, A. De Luca, and J. T. Chalker, Phys. Rev. X **8**, 041019 (2018).

[85] B. Bertini, P. Kos, and T. Prosen, Phys. Rev. Lett. **121**, 264101 (2018).

[86] C.-J. Lin and O. I. Motrunich, Phys. Rev. B **97**, 144304 (2018).

[87] S. Xu and B. Swingle, arXiv:1802.00801.

[88] S. Gopalakrishnan, Phys. Rev. B **98**, 060302(R) (2018).

[89] P. J. D. Crowley, C. R. Laumann, and S. Gopalakrishnan, arXiv:1809.04595.